ISSN 1674-1056
http://cpb.iphy.ac.cn
http://iopscience.iop.org/cpb
中国物理 B
Chinese Physics
中国物理 Chinese Physics B

Synthesized few-layers hexagonal boron nitride nanosheets

Zhao-Jun Mo(莫兆军), Zhi-Hong Hao(郝志红), Xiao-Jie Ping(平晓杰), Li-Na Kong(孔丽娜), Hui Yang(杨慧), Jia-Lin Cheng(程佳林), Jun-Kai Zhang(张君凯), Yong-Hao Jin(金永昊), Lan Li(李岚)
Citation: Chin. Phys. B . 2018, 27(1): 016102. **doi:** 10.1088/1674-1056/27/1/016102

Journal homepage: http://cpb.iphy.ac.cn; http://iopscience.iop.org/cpb

What follows is a list of articles you may be interested in

Theoretical calculations of structural, electronic, and elastic properties of $CdSe_{1-x}Te_x$: A first principles study

M Shakil, Muhammad Zafar, Shabbir Ahmed, Muhammad Raza-ur-rehman Hashmi, M A Choudhary, T Iqbal
Chin. Phys. B . 2016, 25(7): 076104. **doi:** 10.1088/1674-1056/25/7/076104

Influence of nitrogen and magnesium doping on the properties of ZnO films

Dong-hua Li(李东华), Hui-Qiong Wang(王惠琼), Hua Zhou(周华), Ya-Ping Li(李亚平), Zheng Huang(黄政), Jin-Cheng Zheng(郑金成), Jia-Ou Wang(王嘉鸥), Hai-jie Qian(钱海杰), Kurash Ibrahim(奎热西), Xiaohang Chen(陈晓航), Huahan Zhan(詹华瀚), Yinghui Zhou(周颖慧), Junyong Kang(康俊勇)
Chin. Phys. B . 2016, 25(7): 076105. **doi:** 10.1088/1674-1056/25/7/076105

Comparative study on beryllium and magnesium as a co-doping element for ZnO:N

Yu-Quan Su(苏宇泉), Ming-Ming Chen(陈明明), Long-Xing Su(苏龙兴), Yuan Zhu(祝渊), Zi-Kang Tang(汤子康)
Chin. Phys. B . 2016, 25(6): 066106. **doi:** 10.1088/1674-1056/25/6/066106

Van der Waals heterostructure of phosphorene and hexagonal boron nitride: First-principles modeling

Peng Zhang(张鹏), Jing Wang(王静), Xiang-Mei Duan(段香梅)
Chin. Phys. B . 2016, 25(3): 037302. **doi:** 10.1088/1674-1056/25/3/037302

In-situ wafer bowing measurements of GaN grown on Si (111) substrate by reflectivity mapping in metal organic chemical vapor deposition system

Yang Yi-Bin, Liu Ming-Gang, Chen Wei-Jie, Han Xiao-Biao, Chen Jie, Lin Xiu-Qi, Lin Jia-Li, Luo Hui, Liao Qiang, Zang Wen-Jie, Chen Yin-Song, Qiu Yun-Ling, Wu Zhi-Sheng, Liu Yang, Zhang Bai-Jun
Chin. Phys. B . 2015, 24(9): 096103. **doi:** 10.1088/1674-1056/24/9/096103

Synthesized few-layers hexagonal boron nitride nanosheets*

Zhao-Jun Mo(莫兆军)[1,†], Zhi-Hong Hao(郝志红)[2], Xiao-Jie Ping(平晓杰)[1], Li-Na Kong(孔丽娜)[1], Hui Yang(杨慧)[1], Jia-Lin Cheng(程佳林)[1], Jun-Kai Zhang(张君凯)[1], Yong-Hao Jin(金永昊)[1], and Lan Li(李岚)[1]

[1] *School of Material Science and Engineering, National Demonstration Center for Experimental Function Materials Education, Key Laboratory of Display Materials and Photoelectric Devices of Ministry of Education of Ministry of Education, Key Laboratory for Optoelectronic Materials and Devices of Tianjin, Tianjin University of Technology, Tianjin* 300191, *China*

[2] *Tianjin Vocational Institute, Tianjin* 300191, *China*

(Received 13 August 2017; revised manuscript received 13 October 2017; published online 28 November 2017)

The hexagonal boron nitrides (BNs) with different morphologies are synthesized on a large scale by a simple route using a two-step synthetic process. The morphology of h-BN can be easily controlled by changing the heat-treatment atmosphere. The whiskers with 0.5–10 μm in diameter and 50–100 μm in length consist of few-layers nanosheets in the NH_3 gas. The BN nanosheets can be dissociated from the whiskers by ultrasonic treatment, which are less than 5 nm in thickness and even only two layers thick. The concentration and activity of N play an important role, and abundant N and higher activity are conducive for refining grain in reaction. The H_3BO_3 and $C_3N_6H_6$ molecules form a layer-like morphology with the interlinked planar triangle by a hydrogen-bonded structure.

Keywords: boron nitride, few layers, nanosheets

PACS: 61.72.uj, 73.90.+f, 62.23.Kn **DOI:** 10.1088/1674-1056/27/1/016102

1. Introduction

Hexagonal boron nitride (h-BN) consists of alternating sp^2 hybridized B and N atoms within a single layer and weak Van de Waals interaction between stacking multilayers. It has attracted increasing interest in the past few years, due to potential expansive applications in many fields, such as deep transparent membranes, ultraviolet light emitters, protective coatings, and dielectric layer.[1–3] The properties of nanomaterials have very close relationship with its morphology, and to a great extent determine the scope of practical application. All kinds of morphologies of BN were synthesized such as submicron spherical,[4] nanosheets,[5,6] nanotubes,[7,8] collapsed nanotubes,[9] nanofibers,[10] monolayer film,[11] etc.

The BN nanosheets (BNNSs) consist of few-layers h-BN planes, which are an important category of inorganic layered material.[12–14] Compared with graphene, BNNS has relatively high in-plane thermal conductivity (approximately 400 $W{\cdot}m^{-1}{\cdot}K^{-1}$ for few-layer), wide energy band gap, excellent dielectric performance, electrical insulation[15–17] and chemical stability, high resistance to oxidation, mechanical robustness, and good optical properties.[18–20] Few-layers h-BN has been made by a variety of preparation methods. The BNNS was first isolated by micromechanical cleavage using adhesive tape to peel off BN layers from h-BN powder.[21] Solution exfoliation is another method, and BN layers were exfoliated from h-BN flakes using sonication in the presence of polar solvents and/or reagents.[22–24] Laser ablating can also obtain BNNS by an h-BN target.[25] Chemical routes have significant advantages for obtaining large-area h-BN films. The synthetic routes were the reactions of boron oxides with urea,[26] boron oxides with melamine,[27] and boric acid with melamine.[28] The source of nitrogen is far more than the boron source in these routes. The monolayer and few-layers BNNS have been prepared by chemical vapor deposition (CVD) on metal or graphene substrates, in which the thermal decomposition of the amineboranes, ammonia-boraneand borazine are used,[29–31] and the plasma-induced reactions of BF_3 in an H_2/N_2 atmosphere.[32] However, the large scale fabrication of BN nanosheets with a large percentage of single or few layer products is still a challenge. The experimental difficulties and intrinsic insulating character of BN notably depress research enthusiasm with respect to h-BN nanoderivatives.

Here, we synthesize the few-layers h-BN on a large scale by a three-step process with using H_3BO_3 and $C_3N_6H_6$ as the source. The H_3BO_3 and $C_3N_6H_6$ molecules form a layer-like morphology using the interlinked planar triangular by a hydrogen-bonded structure. The few-layers h-BN nanosheet is less than 5 nm thick and consists of even only two layers of h-BN achieved by ultrasonic treatment from the crippled h-BN whisker.

2. Experiment

We describe a simple route to synthesize BN by a two-step synthetic process. Firstly, the H_3BO_3 was dissolved in 150-ml distilled water and heated at 95 °C. Next, $C_3N_6H_6$was added into the dissolved H_3BO_3 and it was kept for 12 h, then

*Project supported by the National Natural Science Foundation of China (Grant No. 11504266), the Tianjin Natural Science Foundation, China (Grant No. 17JCQNJC02300), and the National Key Foundation for Exploring Scientific Instrument, China (Grant No. 2014YQ120351).

†Corresponding author. E-mail: mzjmzj163@163.com

© 2018 Chinese Physical Society and IOP Publishing Ltd

naturally cooled to room temperature. The white precursor was obtained by being filtered and dried at 120 °C for 3 h. Secondly, in order to produce BN, the precursor was treated through a multiple-time heating process. The white precursors were first pre-treated at 500 °C for 3 h in air and then heated at 800 °C for 2 h in a flow of N_2 (0.3 L/min); finally, they were heated to 1000, 1200, and 1500 °C for 2 h under different gas atmospheres (Ar, N_2, and NH_3) with a flow of 0.2 L/min. The method can produce high yield and high purity of the resulting material, which is particularly useful for future commercial applications.

The structure of the BN was investigated by x-ray diffraction (XRD) with Cu Kα radiation at room temperature. The field emission scanning electron microscopy (SEM, HitachiS-8010) and high-resolution transmission electron microscopy (HRTEM, Tecnai F20, Philips, Netherlands) were used to characterize the structure and morphology. Fourier transform infrared (FTIR) spectra (a Nicolet 7100 spectrophotometer) were used to analyze the process. X-ray photoelectron spectroscopy (XPS) (VGESCALAB MKII instrument with Mg Kα ADES source) and an electron energy loss spectrometer (EELS) were used to perform elemental analysis.

3. Result and discussion

3.1. Control of BN morphology

The heated environment plays an important role in the final morphology of the BN, and the transition process of morphology changes with heated gas. Figures 1(a)–1(c) show typical SEM images of BN treated under different heating conditions. Figures 1(a_1)–1(c_1) show the morphologies of the products formed at 1000 °C in the Ar, N_2, and NH_3 gas atmosphere, respectively. In the Ar gas, it is obviously observed that the particles are whiskers in shape and have rough surfaces. In the N_2 gas, the surface of a whisker is also rough and smaller in size. The surface of the whisker remains smooth in the NH_3 gas compared with in the Ar and N_2 gas. When the heated temperature increases to 1200 °C, the whisker consists of nanoparticles with $\sim$ 50 nm in the Ar gas, and the size of nanoparticles is $\sim$ 20 nm in the N_2 gas as shown in Figs. 1(a_2) and 1(b_2). The smooth surface of the whisker is only observed in the NH_3 gas as shown in Fig. 1(c_2). The difference in morphology can be more obviously observed at higher heating temperature (1500 °C). Figures 1(a_3) and 1(b_3) show that the whisker consists of nanosheets, of which the diameter is 200–400 nm and the thickness is about 50 nm in the Ar gas; the diameter of nanosheet is reduced to 100–200 nm with a thickness of 30 nm in the N_2 gas. In the NH_3 gas, the diameter of nanosheet is 100–200 nm, but the thickness is only a few nanometers as shown in Fig. 1(c_3). The different morphologies of BN are synthesized under different atmospheres, because the N_2 and NH_3 participate in the reaction. As is well known, BN can be synthesized using B_2O_3 in the N_2 or NH_3 atmosphere. When B ions do not completely form the stable B–N with N ions (existing dangling bond), it is very easy to combine with oxygen ions to form B–O,

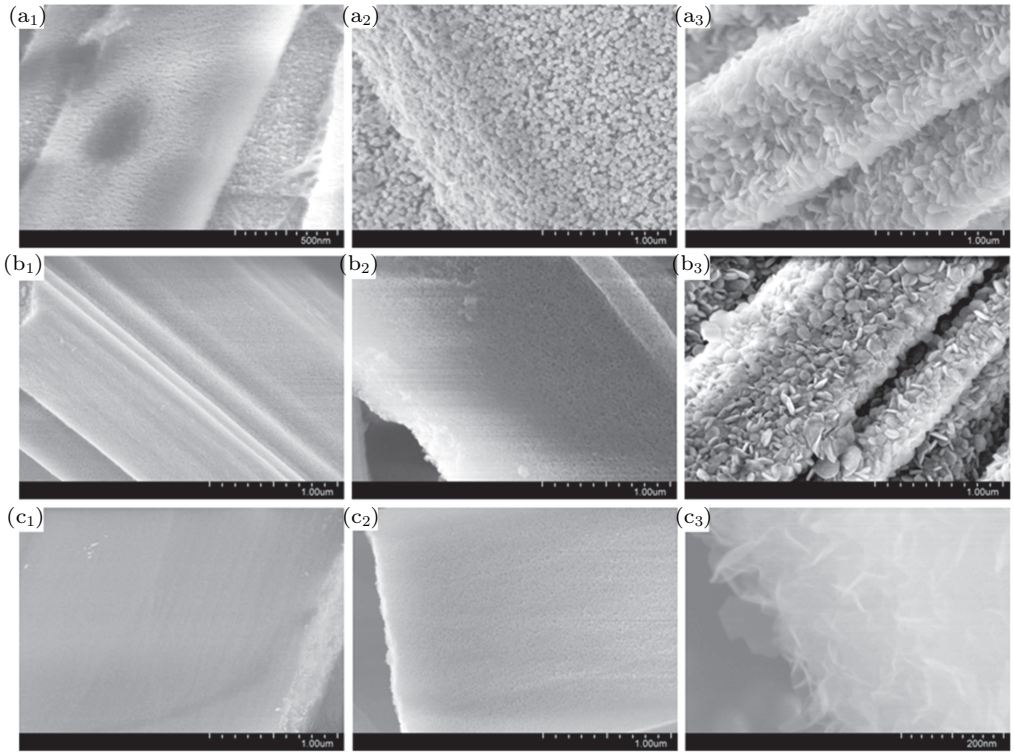


Fig. 1. Typical SEM images of BN treated under different heating conditions: (a_1)–(a_3) 800 °C, 1200 °C, 1500 °C in Ar gas; (b_1)–(b_3) 800 °C, 1200 °C, 1500 °C in N_2 gas; (c_1)–(c_3) 800 °C, 1200 °C, 1500 °C in NH_3 gas.

which is not conducive to the formation of nanoflake. When there is an extra source of N supplement, the dangling bond of B will combine with N ions to form reduced thickness of BN nanosheets. Therefore, the concentration and activity of N ions are important for the reaction process, which maybe affect the process of crystallization. The abundant N may refine grain; the higher activity probably is the significant reason for forming less layer BN nanosheets.

Figure 2 shows XRD patterns of the calcined products prepared at different temperatures and in different atmospheres. The (002) peak of BN and peaks of H_3BO_3 are observed for the heating temperature of 800 °C in N_2 as shown in Fig. 2(a), which indicates that the BN has begun to form (the precursor is heated at 500 °C in air in order to remove part of the carbon ions). The content of H_3BO_3 decreases and completely disappears with increasing the heating temperature in Ar and N_2 atmosphere as shown in Figs. 2(b) and 2(c). When the samples are calcined at 1500 °C, all diffraction peaks should be calculated as a hexagonal BN with lattice parameters of $a = 0.2504$ nm, $b = 0.2504$ nm, and $c = 0.6656$ nm, and the results are well consistent with those reported in (PDF No. 34-0421). However, when the samples are calcined in NH_3 atmosphere, the peak of H_3BO_3 is observed only at 1000 °C in Fig. 2(d). It should be noticed that the full width at half maximum (FWHM) is broader than synthesized in Ar and N_2 atmosphere, which indicates that the grain size decreases. The grain size of the BN can be calculated from the major diffraction peak of (002) using Scherrer formula $D = K\lambda/B\cos(\theta)$, where K is a constant (0.89) and λ is the wavelength of Cu Kα radiation (0.154056 nm). The grain sizes of the BN are 27, 23.2, and 2.2 nm for synthesizing in Ar, N_2 and NH_3 atmosphere, respectively. It indicates that the content of N and the higher activity play an important role and abundant N is conducive to refining grain in reaction.

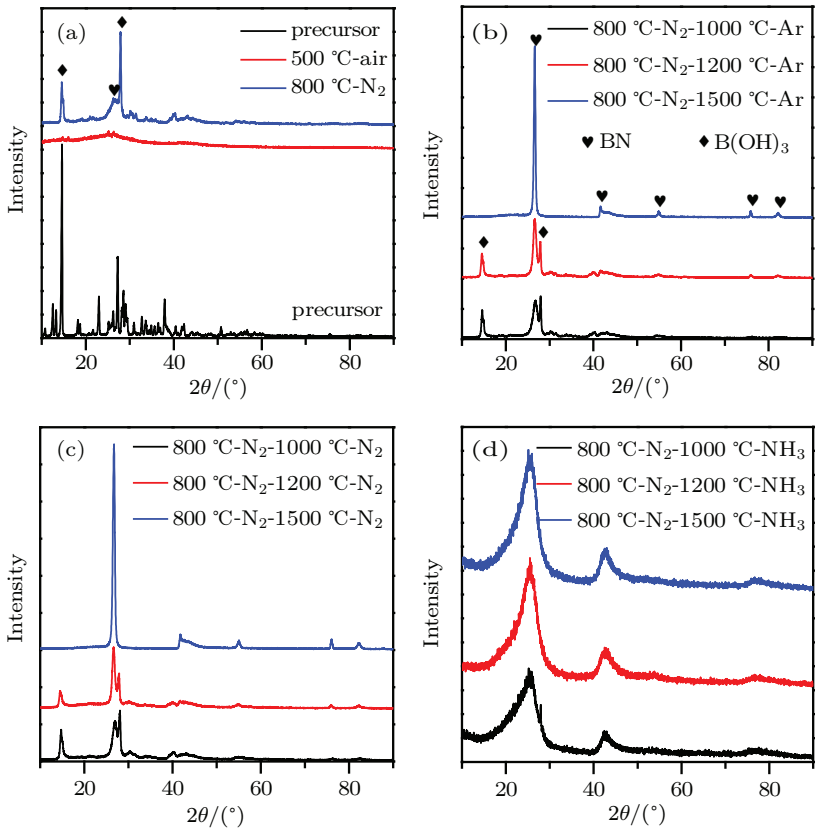


Fig. 2. (color online) XRD patterns of the calcined products at different temperatures and in different atmospheres.

In order to further confirm the effect of different gas on the synthesis of the BN, the x-ray photoelectron spectroscopy (XPS) spectra are measured. Figure 3 shows the XPS spectra of the BN, and the binding energies of B_{1s} and N_{1s} peaks are corrected with respect to the binding energy of the C_{1s} peak (C–C bond) at 284.5 eV. Figure 3(a) shows high resolution B_{1s} spectrum of BN synthesized in Ar atmosphere, which can be fitted with two peaks at 190.33 and 191.14 eV; the B_{1s} spectrum of BN synthesized in N_2, can be fitted with two peaks at 190.34 and 191.18 eV; the B_{1s} spectrum of BN synthesized in NH_3 can be fitted with two peaks at 190.79 and 191.25 eV. The lower energy peak is related with the hexagonal B–N bonding, and the higher energy is the characteristic peak of B–O. The high resolution N_{1s} spectrum of BN can also be fitted with two peaks at 398.18 and 399.25 eV in Ar atmosphere; 398.3 and 399.65 eV in N_2; 398.44 and 400.13 eV in NH_3 atmosphere.

The lower energy peak related with the hexagonal B–N bonding, and the higher energy is the characteristic peak of N–O. There are no impurities such as H_3BO_3 and B_2O_3, when the samples are calcined at 1500 °C, all diffraction peaks of XRD belong to h-BN, which indicates that the oxygen atoms are in the form of BNO. The oxygen concentration of BN synthesized in NH_3 atmosphere is lower than synthesized in Ar and N_2 atmosphere due to the higher activity of NH_3. The stoichiometric ratio of B/N is calculated from our XPS survey to be 1.05, close to a perfect value of 1:1.

For the formation process of BN, the FTIR analyses of the precursor and the products heat treated at different temperatures and gas as shown in Fig. 4. The peaks of 668, 2340, and 2360 cm^{-1} belong to CO_2 absorbed on the surface in all samples. Comparing with the H_3BO_3 and $C_3N_6H_6$, there are various organic groups that involve –NH_2($\sim$ 3400 cm^{-1}), –OH ($\sim$3200 cm^{-1}), N–H ($\sim$ 2900 cm^{-1}), C=N (1635 and 1543 cm^{-1}), C–N (810 and 1238 cm^{-1}), and ν(BO) ($\sim$ 1454 cm^{-1}), HBO_2 ($\sim$ 1040 and 1090 cm^{-1}), B–N (1380 cm^{-1}) in the white precursor. The H_3BO_3 and $C_3N_6H_6$ molecules form a layer-like morphology using the interlinked planar triangle by a hydrogen-bonded structure.[34] The peaks of –NH_2 and –OH are moved with the ligand changing; the C=N (1543 cm^{-1}) and ν(BO) ($\sim$ 1454 cm^{-1}) disappear;

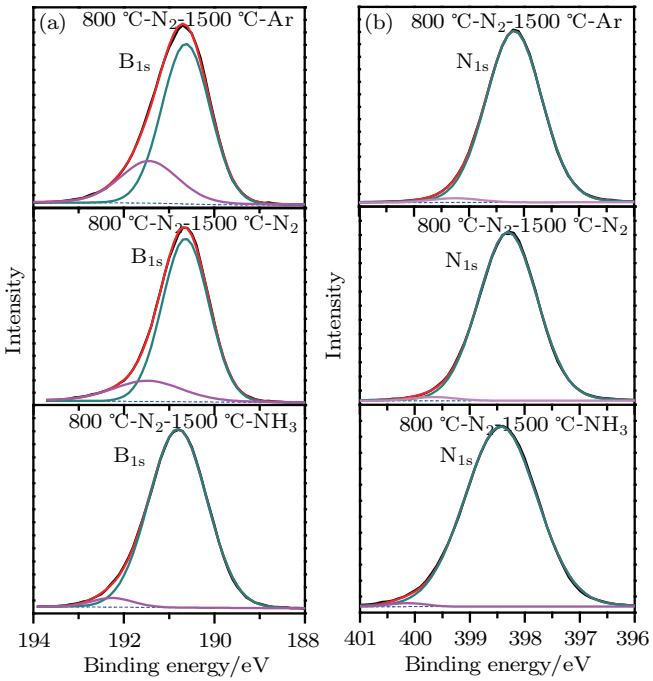


Fig. 3. (color online) XPS deconvolution spectra of h-BN treated under Ar gas, N_2 gas, and NH_3 gas at 1500 °C: (a) B_{1s}; (b) N_{1s}.

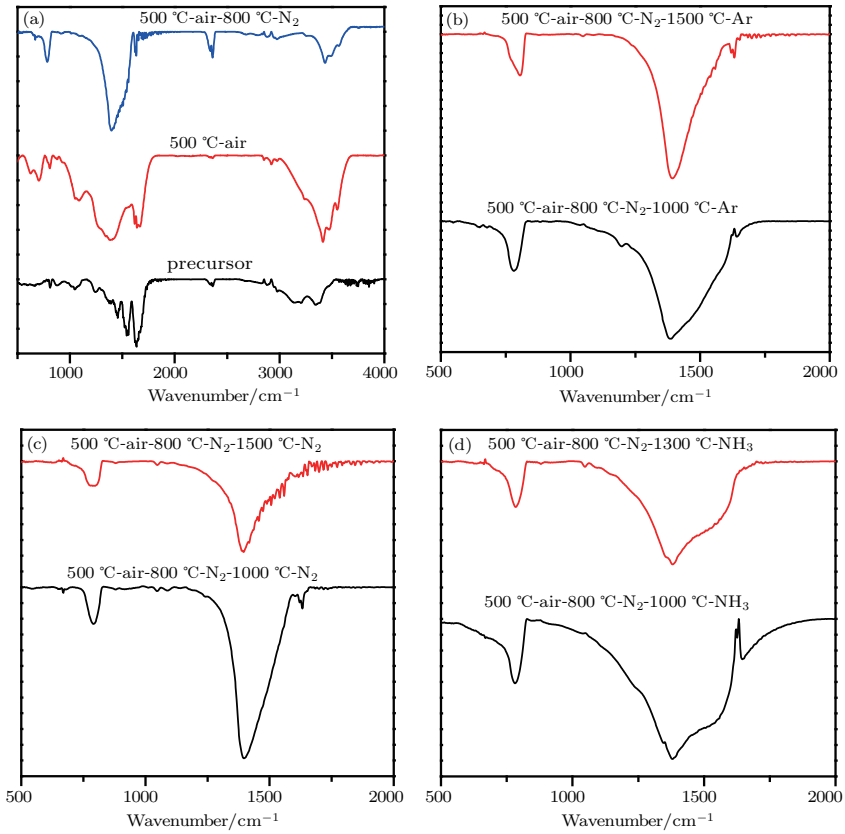


Fig. 4. (color online) FTIR spectra of the precursor and the calcined products in different temperatures and in different atmosphere.

HBO_2 ($\sim$ 1040 and 1090 cm^{-1}) improves and appears at 622 and 702 cm^{-1} corresponding to –BO_3 and B–O–B when being heated at 500 °C in air. Most of the organic groups are eliminated, and the typical absorption bands of h-BN (780 and 1390 cm^{-1}) belonging to B–N–B and B–N are very obvious, when being heated at 800 °C in N_2 gas as shown in Fig. 4(a).

It indicates that the substituted groups are eliminated and B–N and B–N–B bonds of BN form at 800 °C in N_2 gas. When the sample is heated at 1000 °C in Ar, N_2, and NH_3 gas as shown in Figs. 4(b)–4(d), only the peaks belonging to the bonds of B–O, HBO_2, C=N, B–N, and B–N–B are observed. Finally, only the B–N and B–N–B are observed when being heated at 1500 °C. It indicates that the obtaining of perfect BN crystals needs higher temperature.

The concentration and activity of N ions play an important role in the final morphology of the BN according to the results. Although the B–N and B–N–B bonds of BN form at 800 °C in N_2 gas, B ions do not completely form the stable B–N with N ions, some $–BO_3$ and B–O–B remain there. The interaction between the layers of BN is weak Van de Waals, but when there exist oxygen ions, which is good for BN growing along the direction of the *c* axis. The BN nanocrystalline (growth site) is disorderly attached by the impurity (boric acid), which is not good for the growing of two-dimensional materials. That is why the whisker consists of nanosheets. When the samples are calcined at 1500 °C, there is no additional nitrogen source, which only reduces the oxygen concentration of BN in Ar. Although the N_2 can react with B–O, it just prevents BN from further growing and reduces the size of BN due to the low activity of N_2. However, the NH_3 has higher activity, which supplies an extra source of N, surrounding the B–O and prevents BN from further reacting. The oxygen concentration of BN is lower in NH_3 than in Ar and N_2. Additionally, N ions can create interstitials in h-BN in addition to vacancies,[31] which indicates the N ions can enter into the layer between the BN, breaking the weak Van de Waals and similar exfoliation. Therefore, the concentration and activity of N ions are important for the reaction process, affecting the process of crystallization.

3.2. Few-layers h-BN

The crippled surfaces with the protruding edges can be clearly observed by TEM, which reveal that the whisker is assembled by the few-layers nanosheets at 1500 °C in NH_3 gas, as shown in Fig. 5(a). It displays the nanosheets with open edges and the inner interlinked layers. Few-layers h-BN is synthesized by being mechanically tattered from the crippled h-BN whisker using an ultrasonication method as shown Fig. 5(b). The thickness of nanosheets is less than 5 nm (about ten layers thick) and a high-resolution TEM image shows a two-layer nanosheet and the interlayer distance is 0.35-nm characteristic of *d*(0002) spacing in a hexagonal BN, which indicates that the BN layers are well crystallized (see Fig. 5(d)). The EELS analyses clearly show the K-shell excitation shells of B ion (188 eV, B K edge) and N ion (401 eV, NK edge) for a single nanosheet as shown in the insert of Fig. 5(d). The sharp π^* and σ^* peaks of the B and N K edges are typical for the sp^2 bonding configuration,[33] which are characteristics of B and N atoms of the layers.

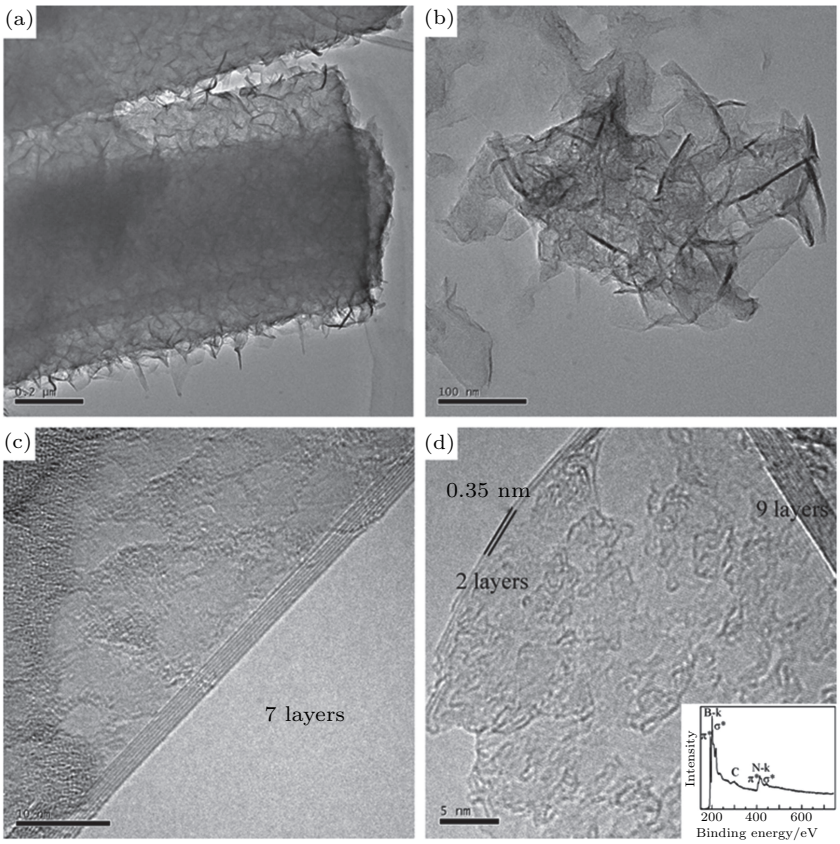


Fig. 5. (a) Typical TEM images of the BN whisker synthesized in NH_3; (b) TEM images of the BN nanosheets synthesized by ultrasonic treatment; (c) and (d) the corresponding HRTEM image and the inset shows the electron energy loss spectrum data acquired for the same sample.

4. Conclusions

The h-BN can be synthesized on a large scale by a simple route using a two-step synthetic process. The morphology of h-BN can be easily controlled by the heat-treatment atmosphere. The BN whisker consists of nanosheets with the diameters of 100–200 nm and the thickness of few nanometers, prepared in the NH_3 gas. The H_3BO_3 and $C_3N_6H_6$ molecules form a layer-like morphology using the interlinked planar triangle by a hydrogen-bonded structure. Organic groups can be absolutely eliminated and B–N bonds basically form at 800 °C, and to obtain the perfect crystals of h-BN the temperature must be as high as 1500 °C. The concentration and activity of N ions play important roles, abundant N ions and higher activity are good for refining grain in reaction. The few-layers h-BN nanosheets less than 5 nm in thickness are synthesized by ultrasonic treatment.

References

[1] Ci L, Song L, Jin C, *et al*. 2010 *Nat. Mater.* **9** 430
[2] Britnell L, Gorbachev R V, Jalil R, *et al*. 2012 *Nano Lett.* **12** 1707
[3] Orofeo C M, Suzuki S and Hibino H 2014 *J. Phys. Chem. C* **118** 3340
[4] Tang C C, Bando Y and Golberg D 2002 *Chem. Commun.* 2826
[5] Golberg D, Bando Y, Huang Y, *et al*. 2010 *ACS Nano.* **4** 2979
[6] Lin Z Y, Liu C R and Chai Y 2016 *2D Mater.* **3** 041009
[7] Chopra N G, Luyren R J, Cherry K, *et al*. 1995 *Science* **269** 966
[8] Dmitri G, Bando Y, Tang C C and Zhi C Y 2007 *Adv. Mater.* **19** 2413
[9] Tang C C, Bando Y, Ding X X, Qi S R and Golberg D 2002 *J. Am. Chem. Soc.* **12** 414550
[10] Qiu YJ, Yu J, Rafique J, Yin J, Bai X D and Wang E G 2009 *J. Phys. Chem. C* **113** 11228
[11] Wu C P, Soomro A M, Sun F P, *et al*. 2016 *Sci. Rep.* **6** 34766
[12] Pakdel A, Bando Y and Golberg D 2014 *Chem. Soc. Rev.* **43** 934
[13] Zeng H B, Zhi C Y, Zhang Z H, Wei X L, Wang X B and Guo W L 2010 *Nano Lett.* **10** 5049
[14] Lei W, Portehault D, Liu D, Qin S and Chen Y 2013 *Nat. Commun.* **4** 1777
[15] Pakdel A, Zhi C, Bando Y and Golberg D 2012 *Materials Today* **15** 256
[16] Jo I, Pettes M T, Kim J, Watanabe K, Taniguchi T and Yao Z 2013 *Nano Lett.* **13** 550
[17] Shen L, Zhao Y, Wang Y, Song R, Yao Q and Chen S 2016 *J. Mater. Chem. A* **4** 5044
[18] Zhi C Y, Bando Y, Tang C C, Kuwahara H and Golberg D 2009 *Adv. Mater.* **21** 2889
[19] Hu S, Lozada-Hidalgo M, Wang F C, *et al*. 2014 *Nature* **516** 227
[20] Lee C, Li Q, Kalb W, Liu X Z, Berger H, Carpick R W and Hone J 2010 *Science* **328** 76
[21] Pacile D, Meyer J C, Girit C O and Zettl A 2008 *Appl. Phys. Lett.* **92** 133107
[22] Han W Q, Wu L, Zhu Y, Watanabe K and Taniguchi T 2008 *Appl. Phys. Lett.* **93** 223103
[23] Lin Y, Williams T V, Xu T B, Cao W, Elsayed Ali H E and Connell J W 2011 *J. Phys. Chem. C* **115** 2679
[24] Lin Y, Williams T V and Connell J W 2010 *J. Phys. Chem. Lett.* **1** 277
[25] Zhang H X, Sajjad M and Feng P X 2010 *Mater. Res. Soc. Symp. Proc.* **1259** 10
[26] Nag A, Raidongia K, Hembram K P S S, Datta R, Waghmare U V and Rao C N R 2010 *ACS Nano* **4** 1539
[27] Gao R, Yin L, Wang C, *et al*. 2009 *J. Phys. Chem. C* **113** 15160
[28] Zhu Y, BandoY, Yin L and Golberg D 2006 *Nano Lett.* **6** 2982
[29] Ci L, Song L, Jin C, *et al*. 2010 *Nat. Mater.* **9** 430
[30] Song L, Ci L, Lu H, *et al*. 2010 *Nano Lett.* **10** 3209
[31] Shi Y, Hamsen C, Jia X, *et al*. 2010 *Nano Lett.* **10** 4134
[32] Qin L, Yu J, Li M, Liu F and Bai X 2011 *Nanotechnology* **22** 215602
[33] Chen Z G, Zou J, Liu G, *et al*. 2008 *ACS Nano* **2** 2183
[34] Roy A, Choudhury A and Rao C N R 2002 *J. Mol. Struct.* **613** 61